ACS Catalysis

Perspective

pubs.acs.org/acscatalysis

Core–Shell Catalysts of Metal Nanoparticle Core and Metal–Organic Framework Shell

Pan Hu, Joseph V. Morabito, and Chia-Kuang Tsung*

Department of Chemistry, Merkert Chemistry Center, Boston College, Chestnut Hill, Massachusetts 02467, United States

ABSTRACT: Encapsulating well-defined nanoparticle catalysts into porous materials to form a core–shell nanostructure can enhance the durability, selectivity, or reactivity of the catalysts and even provide additional functionalities to the catalysts. Using metal–organic frameworks (MOFs) as the encapsulating porous materials has drawn great interest recently because MOFs, as a class of crystalline nanoporous materials, have well-defined pore structures and unique chemical properties. Also, the structures and properties of MOFs are tunable. In this perspective review, we examine recent progress in the development of synthetic methods for metal@MOF core–shell nanostructures as catalysts. Potential directions in the field are also discussed.

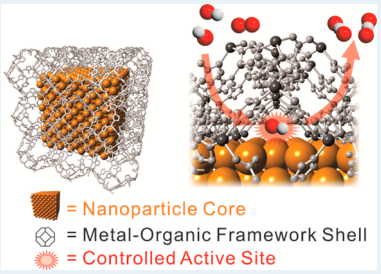

KEYWORDS: *metal nanocrystal, nanoporous material, metal–organic frameworks, core–shell structure, catalysis*

1. INTRODUCTION

Heterogeneous catalysis is at the center of many industrial processes such as oil refining, chemical manufacturing, pollution treatment, and energy conversion.[1,2] Catalysts change the pathways of a chemical reaction, lowering the activation energy and accelerating the reaction rate. Transition metal particles with sizes in the nanoscale have a high percentage of undercoordinated surface atoms and thus can catalyze different reactions. Recent progress in nanotechnology and colloidal chemistry enables new approaches to rationally tune the catalytic properties of metal nanoparticles by providing routes to precisely engineer their structures, including the size, shape, and chemical composition.[3,18−37] A new approach to enhance the performance of a catalyst is to fabricate the nanoparticle catalysts into a core–shell architecture. This type of core–shell nanostructure consists of inner core nanoparticles encapsulated by porous materials. The porous shell materials ensure the accessibility of reactant molecules to the active metal surface and can increase the durability of the catalysts, introduce size selectivity toward different molecules, tune the diffusion rate of the molecules, manipulate the orientation and configuration of the surface molecules, or enrich the reactants on the catalyst surfaces.[4] Various types of metal@porous material core–shell nanostructures have been synthesized with shell materials of silica,[5,6] carbon,[7−10] metal oxides,[11−16] and polymers.[17] As emerging functional materials with modifiable properties, core–shell nanoparticles also find use in many other fields, such as biomedicine and plasmonics.[38−41]

Core–shell catalysts can be categorized based on their structural characteristics. Some of the frequently reported core–shell structures are illustrated in Scheme 1: (a) one core coated by a shell; (b) multiple cores encapsulated in a matrix particle; (c) "yolk–shell" or "bell" structures, consisting of a core encapsulated in a hollow shell with a void in between.[12,17,42−52] Somorjai and co-workers reported the synthesis of Pt@mesoporous SiO_2 core–shell structures, and

Scheme 1. Various Types of Core–Shell Structures[a]

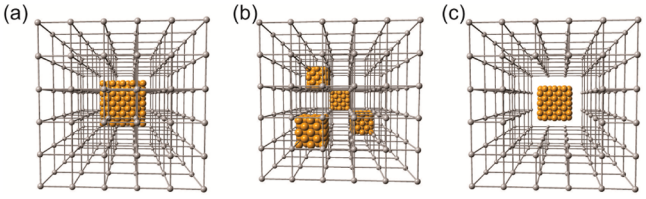

[a](a) Single core–shell structure; (b) multiple cores in one shell structure; (c) yolk–shell structure.

the nanocatalyst exhibits excellent thermal stability in high temperature reactions.[53] Matsumura, Dai, and co-workers reported that Pt and Au nanoclusters encapsulated into a porous carbon shell show activity in catalytic hydrogenation and reduction.[8,10] Metal nanoparticles incorporated in oxides, such as Au@ZrO_2,[54] Au@TiO_2,[55] Ag@CeO_2,[56] and Pd@CeO_2,[57] have also been used as core–shell catalysts. The success in enhancing the catalytic performances of these core–shell nanostructures has inspired scientists to search for more porous materials as the shell materials.

2. METAL@MOF CORE–SHELL NANOSTRUCTURES

Metal–organic frameworks (MOFs), also known as porous coordination polymers (PCPs), are a class of crystalline nanoporous materials with well-defined pore structures and tunable chemical properties.[58−68] MOFs consist of two main components: bridging organic linkers and inorganic secondary building units (SBUs) of metal ions or oxo-clusters. The organic linkers are ditopic or polytopic organic ligands that can bind to metal-containing SBUs to generate crystalline frame-

Received: August 25, 2014
Revised: October 2, 2014
Published: October 7, 2014

   dx.doi.org/10.1021/cs5012662 | ACS Catal. 2014, 4, 4409−4419

work structures with open porosity. The compositions and topologies of MOFs can be vastly varied with over 20,000 different MOFs being reported in the past decades. Compared to pure inorganic nanoporous materials such as aluminosilicate zeolites, MOFs have several unique properties such as the ability to tune the pore size while maintaining the framework topology, known as isoreticularity, adjustable internal surfaces, and modifiable organic linkers. These features endow MOFs with a wide range of functions such as specific molecular adsorptions,[69−78] gas separation[78−82] and sensing,[82−85] drug delivery,[86−89] host−guest chemistry,[90] and heterogeneous catalysis.[91−95] New MOF structures and applications have been extensively explored, leading recently to the commercial production of some MOFs.[96,97] Combining the functions of MOFs with metal cores to create composites is an effective path to multifunctional catalysts. Various nanosized guests have been integrated into MOFs including metal oxide and metal nanoparticles,[98−109] quantum dots,[110−112] polyoxometalates,[113−115] polymers,[116,117] silica,[118−120] carbon nanostructures,[121,122] and biomacromolecules[123,124] for applications such as gas adsorption and storage,[75,122,125] sensing,[126,127] heterogeneous catalysis,[98−102] and molecular release.[87,128] Among these, the encapsulation of metal nanoparticles into MOFs for catalysis has been extensively investigated. Compared with other porous materials, MOFs as a shell material offer unique advantages for catalysis: (i) the nanopores provide confinement effects and shape selectivity;[129,130] (ii) proper organic linkers can offer interaction with nanoparticles;[131] (iii) the great diversity and abundance of MOF structures enables the easy selection of an appropriate MOF as the host matrix; (iv) milder synthetic conditions.

2.1. Overview of Synthesis of Metal@MOF Core−Shell Nanostructures. Two approaches for the encapsulation of nanoparticles into MOFs have been reported. The "ship-in-a-bottle" approach involves the introduction of metal precursors into the presynthesized MOF matrix and the subsequent reduction or decomposition of the precursors to yield metal particles deposited in the cavities. This approach is straightforward, and the pores of the MOFs are used as a template to confine the growth of the nanoparticles to a small size. The interface between the nanoparticles and MOFs produced by this method is relatively simple, but the control of shape and composition of the nanoparticles is challenging. In addition, some of the local framework structure may be damaged during the particle formation, and some particles could undesirably form on the external surface of the MOF crystals. The second approach is the "bottle-around-ship" or *de novo* approach, which involves the assembly of MOF precursors around presynthesized metal nanoparticles. The size, shape, and composition of the nanoparticles can be well-defined and fully preserved during the MOF formation due to the relatively mild MOF synthesis conditions, i.e. compared to zeolites. However, in this approach, the controllable overgrowth of MOFs on nanoparticles rather than self-nucleation is challenging, due to the large interfacial energy barrier between the two materials. Also, the interface between the MOF and the nanoparticles is more complex due to the capping agents on the nanoparticle surface, and the capping agent may hinder the catalytic performance of the nanoparticle core.

2.2. Deposition of Metal Nanocrystals Inside MOF Cavities ("Ship-in-a-Bottle"). Following standards developed for the synthesis of metal@zeolite composites,[132] gas-phase infiltration, solid-state grinding, and liquid-phase impregnation methods were adopted by researchers to deposit metal nanocrystals into the cavities of MOFs. Fischer and co-workers used chemical vapor deposition (CVD) to introduce gas-phase organometallics as the metal precursors.[98,133−140] In a typical synthesis, the chosen MOF is exposed to the vapor of gas-phase organometallic precursors under static vacuum. The volatile precursors diffuse into the pores of the MOFs, and then either hydrogen is introduced to reduce the organometallics or high temperature is applied to thermally decompose the precursors to form metal nanoparticles in the nanopores. Although some of the particles are of sizes larger than the pore size, most of the particle sizes are regulated by the pore confinement. The widely used MOFs in this approach are MOF-5, MOF-177, ZIF-8, and ZIF-90, while the organometallic precursors are (η^3-C_3H_5)Pd-(η^5-C_5H_5), (CH_3)Au(PMe_3), and (η^5-C_5H_5)Cu(PMe_3) for the generation of Pd, Au, and Cu nanoparticles, respectively. Based on the same concept, Haruta and Xu and co-workers developed a solid grinding approach to load metal particles into MOFs.[141−143] Volatile organometallic dimethyl Au(III) acetylacetonate has been used as a metal precursor to deposit Au clusters into different MOFs including MIL-53, MOF-5, and HKUST-1. Surprisingly, this facile and effective method yielded nanoparticles with smaller sizes (∼2.2 nm) than the CVD method, and these nanoparticles exhibited high catalytic activities in oxidation reactions.[141,142]

Although the CVD and solid grinding methods have achieved great success, the precursors are limited to volatile species, and some volatile organometallic precursors are often sensitive to air and water. This can be tackled by utilizing the liquid-phase impregnation method first used by Xu and co-workers.[142,144−147] In a typical synthesis, a porous support is immersed in the solution containing the transition metal precursors, usually in the form of chloride or nitrate salts. The metal ions infiltrate into the pores by capillary force and are subsequently reduced to yield the deposited metal nanocrystals by a reducing agent, typically hydrogen or sodium borohydride. A general drawback of this approach is metal particle formation on the external surface of the MOF crystals. To avoid this problem, Xu's group developed a double solvent method, in which a small amount of aqueous precursor solution is absorbed into the more hydrophilic pores of the employed MOFs, while an excess of organic solvent was introduced to limit the amount of precursors absorbed on the external surface of the MOF crystals, thus minimizing the outside deposition of metal (Figure 1). AuNi@MIL-101 was synthesized by this method and used as catalyst for hydrogen generation from ammonia borane.[147] The morphology and composition control of the nanocrystals is another relatively challenging task in these ship-in-a-bottle approaches. Alloy metal nanoparticles can sometimes be obtained by the coreduction of two different metal precursors, but morphology is not controlled.[147] One of the very few preliminary methods to control these critical parameters was also developed by Xu and co-workers. The formation of shaped bimetallic metal nanocrystals embedded in MIL-101 was achieved by using two organometallic precursors and CO-directed reduction.[148] The preferential binding of CO on 111 facets led to the formation of Pt and Pd polyhedral. The nanocrystals showed metal segregation, with a Pd-rich core and a Pt-rich shell.

Regardless of the general lack of shape and composition control, the ship-in-a-bottle strategy is an efficient way to generate ultrasmall metal nanocrystals in MOFs. Some of the metal nanoparticles might be bigger than the pores but are

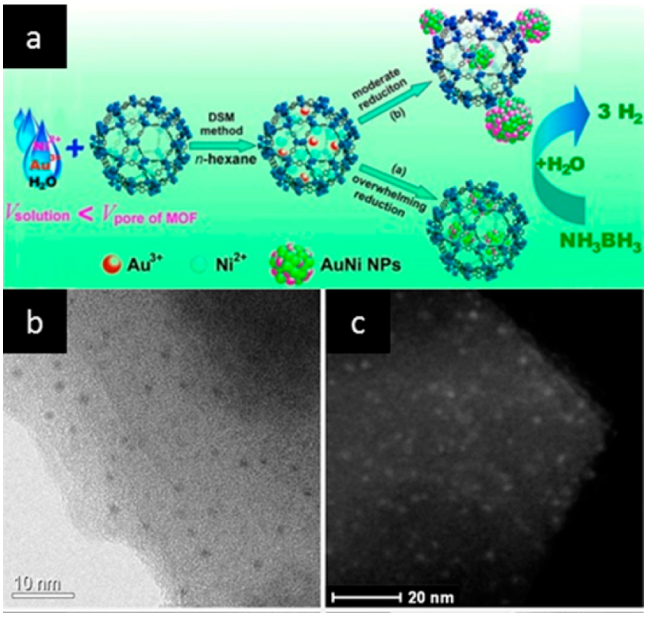

Figure 1. (a) Schematic representation of impregnation of AuNi alloy nanoparticles into MIL-101 matrix by the double solvent method combined with a liquid phase concentration-controlled reduction strategy. (b) and (c) TEM images of AuNi@MIL-101. (Reprinted with permission from ref 143. Copyright ©American Chemical Society 2013.)

generally restrained from growing very big due to confinement by the frameworks. This approach is facile and scalable. Nevertheless, for certain catalytic applications, composition and shape control is more important than ultrasmall nanocrystal sizes. In these reactions, the MOF plays a more important role in interacting with the reactants, products, and intermediates. Therefore, different approaches need to be developed for these applications. Furthermore, the locations of metal particles within the MOF crystal are often random and unpredictable in the ship-in-a-bottle method. The loading amount of metal is also limited, because too much metal will cause the degradation of the MOF matrix.

2.3. Assembly of MOF around Metal Nanocrystals ("Bottle-around-Ship" or "*de Novo*"). Recently, the bottle-around-ship or *de novo* synthetic strategy was used, in which preformed metal nanocrystals are introduced into the precursor solution of a MOF. During the nucleation and growth of MOF crystals, the metal nanoparticles are incorporated into the MOF matrix. The size, shape, chemical composition, and active properties of the metal nanoparticles are preserved after the encapsulation. This approach provides more control in catalytic and optical applications because of the better control of shape and composition of the embedded nanoparticles. Also, the particle sizes are not limited by the MOF pore size. The strategy is straightforward, but many synthetic parameters need to be considered and optimized, including the interactions between the MOF and nanoparticle surfaces, the capping agents on the surface of metal nanoparticles, the interface between the MOF and nanoparticle surface, and the compatibility of the nanoparticles and the MOF synthesis conditions.

Providing a proper interaction between the MOF and nanoparticle surface is the critical parameter of this approach because MOFs tend to self-nucleate and form individual particles rather than overgrow on the metal particles. Sada and co-workers reported the first example of an Au nanorod@$Zn_4O(bpdc)_3$ (IRMOF-9) composite using the bottle-around-ship strategy.[149] The original CTAB capping agent of Au nanorods was first replaced by 11-mercaptoundecanoic acid (MUA) to increase the interaction between the Au surface and the MOF, and then the MUA capped Au nanorods were added into *N,N*-diethylformamide (DEF) solutions containing the MOF precursors, 4,4′-biphenyldicarboxylate (bpdc) and zinc nitrate. Later, Akamatsu and co-workers used a similar concept to synthesize an Au@$Cu_3(btc)_2$ (HKUST-1) composite.[150] Hupp, Huo, and co-workers have made the method more general by using a polymer, polyvinylpyrrolidone (PVP), to mediate the interaction to encapsulate various nanoparticles into ZIF-8 crystals, including metal nanocrystals, magnetic nanoparticles, and quantum dots[151] (Figure 2). The PVP-

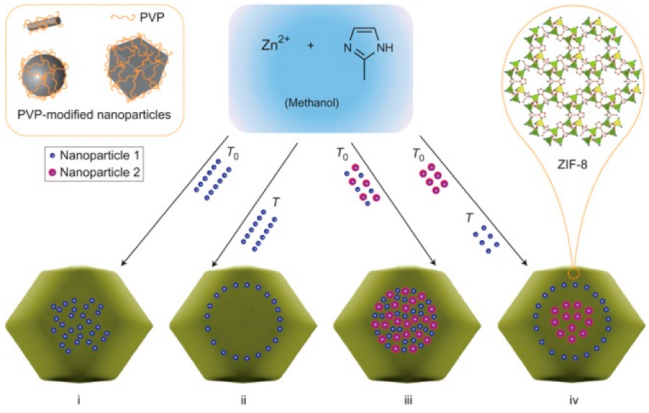

Figure 2. Capped with the surfactant PVP, inorganic nanoparticles of various sizes, shapes, and compositions can be encapsulated into ZIF-8 crystals formed by the assembly of zinc and 2-methylimidazolate in methanol. The spatial distribution of nanoparticles can also be controlled by the adding sequence. (Reprinted with permission from ref 147. Copyright ©Nature Publishing Group 2012.)

capped nanocrystals were mixed with a methanol solution of the ZIF-8 precursors, 2-methylimidazole and zinc nitrate, and then the nanocrystals were encapsulated into ZIF-8 through the adsorption of metal particles on the continuously forming fresh surfaces of the growing MOF spheres. The spatial distribution of encapsulated nanoparticles can be controlled by the adding sequence. In most of these studies, multiple nanoparticles are encapsulated in one MOF crystal (Scheme 1). A configuration of one nanoparticle in one MOF shell could provide a more specific control in certain catalysis applications. By tuning the synthetic conditions of this PVP coating method, Tang and co-workers incorporated single Au and Pd nanoparticle cores into MOF-5 and MOF-3 (IRMOF-3) shells, respectively.[126,152] Recently, metal@MOF yolk−shell structures with a void between core and shell have also been explored; discussion about this type of materials can be found in the perspective part.

Compared with the ship-in-a-bottle deposition of metal precursors into MOF crystals, the *de novo* assembly of MOFs around preformed metal nanocrystals has significant advantages. The nanoparticles are not inside the cavities, and thus the particle size will not be restricted and it will not cause damage to the MOF matrix during the formation of the nanocomposite. The well-developed synthetic methods for metal nanocrystals can be applied to construct particles with a variety of sizes, shapes and compositions. After MOF coating, all of the

dx.doi.org/10.1021/cs5012662 | *ACS Catal.* 2014, 4, 4409−4419

structural features and reactive properties of the nanoparticles are preserved. Also, control over the spatial distribution of the encapsulated nanoparticles such as the configuration of one nanoparticle in one MOF shell can be only achieved in the *de novo* assembly approach. Nevertheless, challenges remain in this strategy. Capping agents are important to avoid the aggregation of particles in solution, and these surfactant or polymer capping agents are used to facilitate the MOF overgrowth; however, due to these capping agents, the interfaces between the MOF and metal surface are relatively complex and ill-defined. An additional challenge is that if the capping agent on the metal surface cannot be effectively removed after the MOF coating, it may negatively affect the catalytic performance. Finally, the structure control in most of these works is not optimized. Either multiple particles were encased in one giant MOF crystal or one particle was surrounded by a polycrystalline MOF shell, which may have defects or cracks.

3. METAL@MOF CORE–SHELL NANOSTRUCTURES IN CATALYSIS

Like most metal oxides in traditional heterogeneous catalysts, the MOF shell could simply serve as a support and help to prevent the aggregation of metal nanoparticles during catalytic reactions. For example, MOFs have been widely studied for the synthesis of small Au nanoparticles (less than 5 nm) within the matrix due to the nanopore confinement.[142] The flexible porous structures of MOFs can impart size-selectivity to the catalyst and can bridge the gap between zeolites and mesoporous materials. In addition, with coordinatively unsaturated metal SBUs and functional groups on the organic linkers, MOF themselves can serve as catalysts and work together with the metal nanocatalysts. Here, we will discuss various catalytic reactions categorized by reaction type (gas-phase, liquid-phase, cascade, photocatalysis) as well as other applications such as molecular sensing and surface enhanced Raman spectroscopy (SERS).

3.1. Gas-Phase Catalysis. CO oxidation is one of the most studied gas-phase catalytic reactions, due to its significance in practical applications such as gas purification, gas sensors, and exhaust treatment. Previous studies show that noble metal nanocrystals with sizes below 5 nm exhibit high activity for CO oxidation, and that as the particle size shrinks, the activity for CO oxidation boosts remarkably.[153] MOFs provide opportunities for the confined synthesis of small metal particles and can serve as a support for metal nanocatalysts. El-Shall and co-workers synthesized Pd@MIL-101 and PdCu@MIL-101 composites with a 2.9 wt % loading that displayed high activity for CO oxidation.[154] Xu and co-workers reported catalytic CO oxidation by Au@ZIF-8 and Pt@MIL-101.[142,148]

Gas-phase size-selective hydrogenation of alkenes is a good model system to demonstrate the size selectivity of the core–shell catalyst. Our group has reported the size-selective hydrogenation of ethylene, cyclohexene, and cyclooctene[155] (Figure 3). Pd@ZIF-8 core–shell catalysts were compared with control catalysts consisting of Pd deposited on the external surface of ZIF-8. All of the catalysts showed high activity and similar activation energies for ethylene hydrogenation, while the core–shell catalysts showed no detectable activity for cyclooctene hydrogenation. This result clearly demonstrates the molecular size-selective property of the ZIF-8 shell: that ethylene molecules (2.5 Å; kinetic diameter: 3.9 Å) are small enough to diffuse through the pore aperture (3.4 Å) while the cyclooctene molecules (5.5 Å; kinetic diameter: 6.4 Å) are excluded. A point worth emphasizing is that, in contrast to the more rigid zeolites, the aperture sizes of MOFs derived from X-ray crystallography are not the ultimate limit because of framework flexibility, and thus molecules with sizes slightly larger than the aperture size can also pass through the frameworks.[156] No significant deactivation was observed even when the catalysts were heated to 150 °C. Somorjai, Yaghi, and co-workers studied the gas-phase hydrogenative conversion of methylcyclopentane catalyzed by Pt nanocrystals embedded in single crystalline UiOs that exhibits unique product selectivity for C_6-cyclic hydrocarbons.[157]

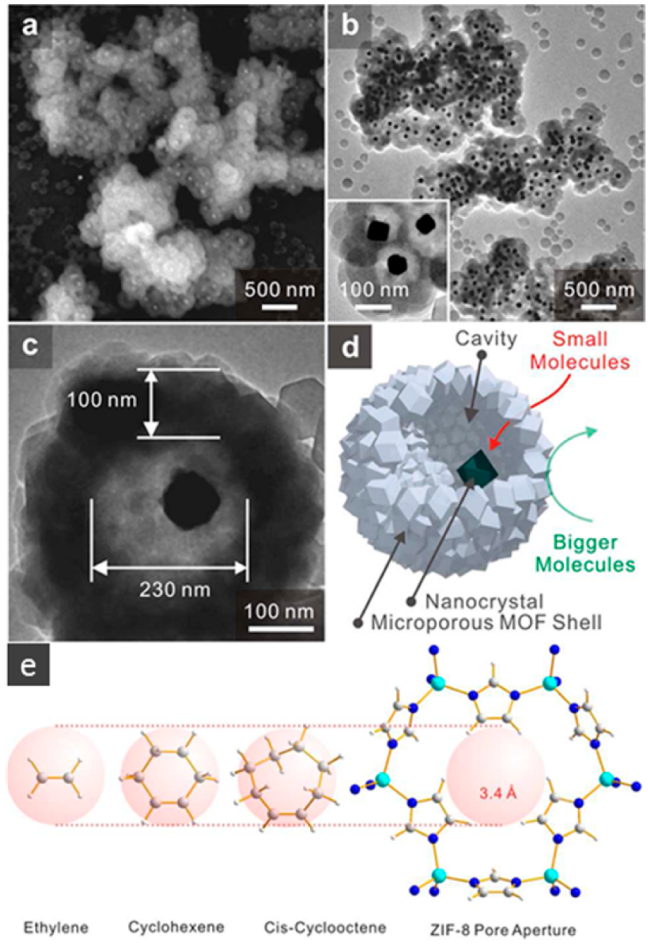

Figure 3. (a), (b), (c), and (d) SEM and TEM images and the schematic of Pd nanocrystals encapsulated into polycrystalline ZIF-8 yolk–shell structures. (e) Molecular size selective catalytic hydrogenation reactions. (Reprinted with permission from ref 152. Copyright ©American Chemical Society 2012.)

The examples show that MOFs are good templates for the preparation of highly active metal nanocrystals and are robust catalyst supports for reactions requiring relatively lower temperatures, with the benefits of reactant enrichment and molecular size selectivity. It is worth noting that although many MOFs exhibit excellent thermal stability, in some cases up to 500 °C,[158] they are still not competitive with zeolites, the most-widely used commercial catalyst, in harsh reactive conditions. Therefore, MOF-based catalysts are more suitable for industrial applications with high-value-added products such as fine chemicals manufacturing.

3.2. Liquid-Phase Catalysis. The framework encapsulation of molecular catalysts has been vastly studied for liquid-phase

dx.doi.org/10.1021/cs5012662 | ACS Catal. 2014, 4, 4409–4419

catalysis;[91] however, molecular catalysts are not our focus here. A variety of liquid-phase catalytic reactions have been conducted using metal@MOF composites such as aerobic alcohol oxidation, selective alkene hydrogenation, formic acid dehydrogenation, C−C bond coupling, and ammonia borane hydrolysis. As a heterogeneous catalyst, metal nanoparticles encapsulated into MOFs offer advantages such as enhanced durability and easier separation and recyclability. As in gas-phase reactions, the nanoporous MOF shell in liquid-phase reactions also prevents aggregation/sintering of metal nanocrystals, helps to concentrate the reactant molecules, and exhibits selectivity toward different molecules. The chemical stability of MOF shells, especially in acidic or moist reaction conditions, needs to be carefully considered when applied to organic reactions. For example, ZIF-8 is highly resistant to boiling alkaline water and organic solvents but is vulnerable to acidic conditions.[61] MOF-5 is thermally stable but can be destroyed by water.[159] The tendency for MOFs to undergo linker exchange in certain solvents should also be considered when designing a reaction, as such reactions may promote leaching of the active species,[160] in particular by opening enlarged cavities in the material by linker dissociation.[161]

ZIF-8 exhibits great performance for liquid-phase catalysis because it has great alkaline chemical stability and its pore structure shows specific molecular sieving behaviors. Huo, Li, and co-workers used the bottle-around-ship approach to prepare a metal@ZIF-8 catalyst that shows size-selective hydrogenation due to the uniform microporous structure, allowing 1-hexene to react while excluding the bulkier *cis*-cyclooctene.[131,151] MIL-101 was chosen as the support in many studies due to the relatively stable structure and the large pore sizes (2.9−3.4 nm) and aperture sizes (1.2−1.4 nm), which facilitated the diffusion of the reactant molecules. Xu and co-workers reported the decomposition of formic acid by bimetallic Au−Pd nanoparticles immobilized in ethylenediamine-grafted MIL-101.[144] The grafted ethylenediamine molecules on the unsaturated Cr^{3+} centers improved the immobilization of the small metal clusters in the pores. The small Au−Pd particles showed strong bimetallic synergistic effects with a higher catalytic performance and tolerance toward CO poisoning. C−C bond couplings such as Suzuki-Miyaura, Ullmann, Heck, and Sonogashira reactions are important in organic synthesis. Pd-catalyzed C−C coupling has been reported using Pd nanoparticles encapsulated into MOFs.[162−164] The Pd@MIL-101 catalyst shows good catalytic activity that is comparable with or even higher than the commercial Pd/C catalyst and is easily recoverable and reusable. Ammonia borane is a promising material for chemical hydrogen storage, from which hydrogen can be released by either hydrolysis or pyrolysis. Xu and co-workers reported that Pt@MIL-101 and AuNi@MIL-101 showed great catalytic performance in the hydrolysis of ammonia borane.[146,147] UiOs are popular candidates for support because of the highly chemical and thermal stability.[165] Huang and co-workers prepared Pt@UiO-66-NH_2 nanostructures by an aqueous ship-in-a-bottle impregnation method and employed them in the chemoselective hydrogenation of cinnamaldehyde in methanol, with ∼90% selectivity for the C═O hydrogenation product over that of the C═C bond.[166] Comparisons with control catalysts of Pt deposited on the external surface of UiO-66-NH_2 particles and of SiO_2 spheres demonstrated that the confinement effects of the MOF nanopores led to the observed selectivity.

3.3. Cascade and Tandem Reactions. Cascade or tandem reactions are consecutive series of catalytic reactions that often proceed via highly reactive intermediates such as radicals, carbenes, or organometallic complexes.[167] The metal@MOF composite could be a powerful platform for cascade catalysis because it can combine the active sites of metal nanoparticles with the intrinsic active sites of MOFs, such as those with coordinatively unsaturated metal nodes or organic linkers with different functional groups (amine, carboxylic, etc.). Tang and co-workers designed a cascade catalyst, consisting of a Pd core and an amino-functionalized IRMOF-3 shell[152] (Figure 4). The

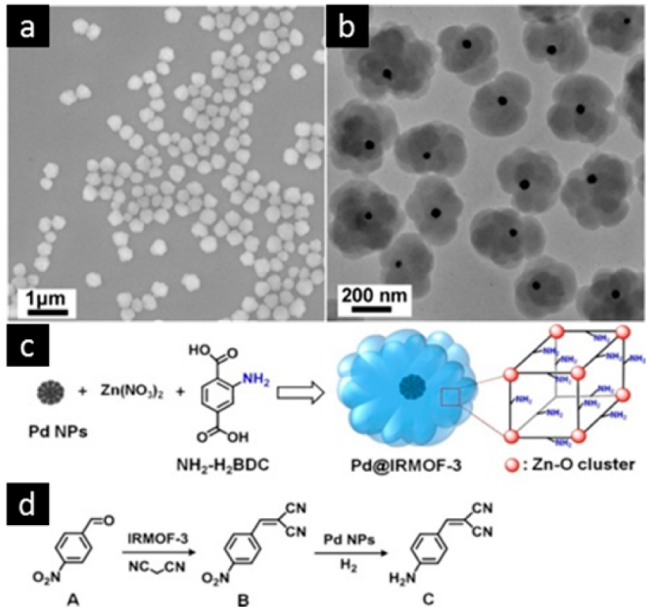

Figure 4. (a) and (b) TEM images of Pd@IRMOF-3 core−shell nanoparticles. (c) Synthetic approach for Pd@IRMOF-3 core−shell nanoparticles. (d) Model cascade reactions of Knoevenagel condensation of 4-nitrobenzaldehyde and malononitrile via the amino-functionalized IRMOF-3 shell and subsequent selective hydrogenation of intermediate B to C via Pd cores. (Reprinted with permission from ref 148. Copyright ©American Chemical Society 2014.)

reaction chosen as a proof-of-concept was a two-step process, consisting of first the Knoevenagel condensation of 4-nitrobenzaldehyde and malononitrile into 2-(4-nitrobenzylidene)malononitrile catalyzed by the basic amino group on the organic linker of the IRMOF-3 shell, followed by the selective hydrogenation of the nitro group to an amine by the Pd core. The Pd@IRMOF-3 core−shell catalyst had better hydrogenation selectivity and stability than a Pd on IRMOF-3 support because of the group-selective adsorption, constant diffusion direction, and matched pore dimensions. The amino groups on the surface of IRMOF-3 exhibited preferential interaction with the nitro group of the reactant, and the reactant molecules preferred entering into the nanopores with the nitro group first. Reactants with shorter carbon chain lengths showed lower selectivity and yield because they can rotate freely within the pores. Li et al. also utilized amine-functionalized UiO-66 with encapsulated Pt nanoclusters for a tandem oxidation-acetalization reaction, which exhibits excellent catalytic activity and selectivity.[168] So far, only few cascade reactions have been reported, but we believe that it is a very promising direction to combine the catalytic activities of

dx.doi.org/10.1021/cs5012662 | ACS Catal. 2014, 4, 4409−4419

both metal core and MOF shell for the design of future multifunctional catalysts.

3.4. Photocatalysis. Solar energy is an ultimate sustainable energy source, and it is crucial to discover efficient and cost-competitive ways to convert the solar energy to chemical energy for the wide-scale utilization of energy from sunlight. MOFs provide an interesting platform to integrate light-harvesting antennae and catalytic centers for solar energy conversion.[169] The encapsulation of molecular photocatalysts in MOFs has been reported previously,[110,170,171] and, therefore, multifunctional composites can be achieved by incorporating metal nanoparticles in these host–guest composites. Both the MOF and the metal particles participate in the photocatalytic reactions, and this composite catalyst is more recyclable and efficient compared with molecular catalysts. Lin and co-workers deposited Pt nanocrystals into the photoactive UiO-type MOFs built from $[Ir(ppy)_2(bpy)]^+$-derived dicarboxylate ligands and $Zr_6(\mu_3\text{-}O)_4(\mu_3\text{–}OH)_4$ secondary building units[172] (Figure 5).

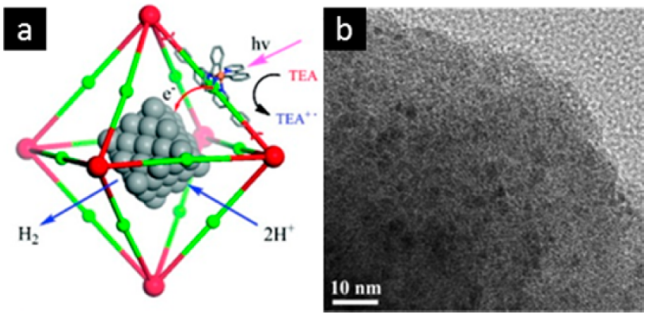

Figure 5. (a) Scheme of Pt nanoparticles loaded into photoactive MOF exhibit effective photocatalytic activities for hydrogen evolution by synergistic photoexcitation of the MOF frameworks and electron injection into the Pt nanoparticles. (b) Corresponding TEM image. (Reprinted with permission from ref 168. Copyright ©American Chemical Society 2012.)

Solar driven hydrogen evolution, one-half of overall photocatalytic water splitting, was carried out over the catalyst. The photoactive MOF served as a phosphor, which can harvest the sunlight, and the embedded metal nanoparticles served as the cocatalyst for hydrogen evolution. The core–shell composite showed higher turnover frequencies and higher turnover numbers than homogeneous controls. The radicals generated in the MOFs (iridium complex molecules) and platinum nanoparticles were believed to facilitate electron transfer between the two species and thus enhance the catalytic activity. The MOF matrix was not only a support for the metal nanoparticles but also an essential participant in the catalytic reaction.

3.5. Spectroscopy and Hydrogen Storage. In addition to catalysis, metal@MOF core–shell structures can also be used in optical sensing applications if metal nanocrystals with unique optical properties are used as core and MOFs with size-selective and adsorptive properties are used as shell. These optical applications can also benefit catalysis as they allow the in situ monitoring of the reaction to study the mechanism and pathway. Sada and co-workers used SERS on Au nanorods encapsulated into MOF-5 and its larger-pore analog $Zn_4O(bpdc)_3$ (IRMOF-9) to in situ monitor guest molecule diffusion and exchange within the framework[127,149] (Figure 6). The crystalline MOF-5 shell demonstrated size selectivity between the SERS substrates pyridine (Py), 2,6-biphenylpyridine

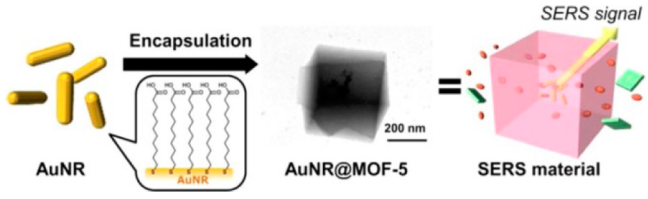

Figure 6. Au nanorods encapsulated in MOF-5 exhibit size-selective SERS signals toward different substrates pyridine (Py), 2,6-biphenylpyridine (BPPy), and poly(4-vinylpyridine) (PVPy). (Reprinted with permission from ref 123. Copyright ©American Chemical Society 2013.)

(BPPy), and poly(4-vinylpyridine) (PVPy). Only Py and BPPy could diffuse to the Au surface and exhibit SERS signals. No signal was detected for PVPy because the molecular size is larger than the pore size of MOF-5. Tang and co-workers used the same concept to study the selective sensing toward CO_2 in a CO_2/N_2 gas stream.[126] The core–shell Au@MOF-5 composite with a shell thickness of 3.2 nm exhibited highly selective sensing toward CO_2 in a CO_2/N_2 gas mixture because the thin shell allowed not only selective enrichment of CO_2 but also maximization of the detected SERS intensity.

Gas storage is another popular application for MOFs that is relevant to catalysis. Several methods[70,73] have been applied to construct MOF-based hydrogen storage materials, including tuning the pore size[173] and generating accessible metal sites.[174,175] Some recent works show that the core–shell structure can benefit gas storage dramatically as well.[69,71,72,176] Pd nanocrystals embedded in MOFs have been shown to be one of the more promising hydrogen storage materials with enhanced capacity.[72,176,177] Kitagawa and co-workers recently reported that MOF-coated Pd nanocrystals showed enhanced hydrogen storage capacity and speed.[75] The MOF they used was $Cu_3(btc)_2$ or HKUST-1, in which the Cu^{2+} was partially reduced while Pd was in a partial oxidation state. The electrons of the Pd nanocubes were partially donated to the HKUST-1 framework, which resulted in an increased number of holes in the 4d band of Pd. This electronic change enhanced the hydrogen storage capacity and the kinetics of hydrogen absorption.

From the examples discussed above, we may conclude that metal@MOF core–shell structures exhibit great potential for many applications, including but not limited to heterogeneous catalysis, spectroscopy, and hydrogen storage. By integrating the unique catalytic and optical properties of metal nanocrystals and the highly porous structures of MOFs, composite nanomaterials with multiple functionalities can be constructed. As promising functional materials, more progress in the field of metal@MOF composites is eagerly expected, such as novel structures, interfacial studies, and new methods to add functionality. Next we will provide several of our prospective directions for this exciting research area.

4. PROSPECTIVE DIRECTIONS

To further improve the catalytic performance of core–shell nanocomposites, it is important to develop new methods to control and rationally design the structures. Here, we propose three interesting prospective directions that could generate impact to the field: yolk–shell structures, crystal structure alignment, and postsynthetic methods to engineer metal@MOF composites.

dx.doi.org/10.1021/cs5012662 | ACS Catal. 2014, 4, 4409–4419

4.1. Yolk–Shell Structures. Yolk–shell structures, or "nano-rattles", which have an interstitial cavity between the metal particle cores and nanoporous shells,[10,15,44,54,57,178,179] could be an interesting candidate for catalysis study. Compared to the core–shell structure, the yolk–shell structure not only exposes more of the core's active surface area to reactant molecules but also makes the interaction of reactant and catalyst more homogeneous. A few pioneering syntheses of metal@MOF yolk–shell structures have recently been reported and the materials applied in heterogeneous catalysis.[155,180,181] Our group introduced the first yolk–shell metal@ZIF-8 nanocomposite by a template synthesis method[155] (Figure 3). Metal nanocrystals of Pd and Au were coated with a layer of Cu_2O as the sacrificial template. By adding the Cu_2O coated metal nanocrystals into solutions containing the MOF precursors, a polycrystalline ZIF-8 shell was generated. The Cu_2O surface provided sites for the nucleation and growth of the ZIF-8 coating layer and was etched simultaneously by the protons generated during the formation of ZIF-8. Huo and co-workers used the same strategy to incorporate various nanoparticles, such as Au NPs, Au nanorods, Pd nanocubes, and Pt-on-Au dendritic nanoparticles, into HKUST-1 to form yolk–shell nanostructures.[180] Cu_2O was used as both the template and source of Cu^{2+} ions. Various inorganic nanoparticles are expected to be incorporated into diverse MOFs by using this sacrificial template method. It could even be possible to generate the core-multiple-shell or "onion" structure by this method, which has been previously achieved in silica.[182] Each layer could consist of different types of MOFs that selectively enrich different reactants or let different molecules pass through. There has been some success in the preparation of yolk–shell metal@MOF composites without the use of sacrificial templates. Wang and co-workers reported the template-free synthesis of hollow MOF nanocages by a solvothermal method.[181] The detailed mechanism of the cavity formation is not clear, but an interesting surface-energy-driven formation mechanism was proposed, in which the MOFs with high surface energy facets were formed first and then dissolution and migration of the inner crystallites occurred to reduce the surface energy. Compared with the template synthesis, this template-free method is more straightforward; however, due to the complicated dissolution and migration process, the surface of the nanoparticles might be more complex. A recent study showed that geometrical frustration can also guide the formation of yolk–shell nanoparticles in the absence of sacrificial templates.[183]

The yolk–shell structure is ideal to encapsulate various inorganic nanoparticles into a void for different functionalities. Besides metal nanocrystals, homogeneous molecular catalysts could also be trapped in the void of yolk–shell structures. A multifunctional yolk–shell nanocatalyst with multiple nanoparticle cores and molecular active species is also anticipated.

4.2. Interface and Alignment. The understanding and engineering of the interface between the metal catalyst core and the nanoporous material shell will be critical to the catalytic performance[31,35,184] because the structure at the interface could change the sorption behaviors of reactant molecules on the catalyst surface which significantly affect the yield and selectivity of the product. However, interfacial control in MOF core–shell nanocomposites is challenging because of the large interfacial energies between materials with crystal lattices in different scales.

An understanding of interfacial chemistry in MOF synthesis is the first step toward interfacial control. Some synthetic works provide intersting hints. De Vos and co-workers developed the interfacial synthesis of hollow MOF capsules.[185] The HKUST-1 precursors in two different solvents were delivered together, in which aqueous droplets containing the metal source were generated in the coflowing water-immiscible alcohol containing the organic linker. The coordination reaction was thus only allowed at the interface of the two solvents, resulting in the formation of hollow HKUST-1. Huo and co-workers studied the oriented growth of ZIF-8 on a patterned self-assembled monolayer (SAM) on an Au (111) surface.[186] The Au (111) substrate was covered by a SAM of 1-octadecanethiol (ODT), and the rest of the area was passivated by 16-mercaptohexadecanoic acid (MHA). They found that ZIF-8 preferentially occurred on the low-energy ODT-patterned area rather than the high-energy MHA region. The crystal orientation was affected by the odd–even effect for SAMs. The oriented growth of ZIF-8 only happened on the alkanethiol-functionalized Au surface with C_{12}, C_{16}, and C_{18} carbon chain lengths. The oriented growth of the ZIF-8 crystals was found to result from fast crystallization of the nuclei triggered by the specific SAM surfaces. The studies of liquid–liquid and liquid–solid interface of MOF nucleation and growth provide knowledge of the formation mechanism at molecular level and can be used to guide the future development of MOF composite materials. Recently, our group reported a new proof-of-concept colloidal synthetic method for core–shell composites with controlled alignment between metals and MOFs[187] (Figure 7). The surfactant CTAB was chosen to control the interface and facilitate the overgrowth of ZIF-8 on well-defined Pd and Au nanocrystals. The lattice constants of the precious metal core and the ZIF-8 shell differ by almost an order of magnitude. The metal nanocrystals were individually encased in single crystalline ZIF-8 to generate the core–shell structure in a one-to-one fashion. An alignment between the (100) planes of the metal and the (110) planes of ZIF-8 was observed, demonstrating the first example of lattice alignment between a metal nanoparticle core and a MOF shell. This surfactant-directed overgrowth could be a general method to fabricate various inorganic nanoparticles in MOF core–shell structures with controlled alignments. A detailed mechanistic study is expected by in situ monitoring of the reaction process. The well-aligned metal@MOF structures provide an ideal platform to study molecular orientations in catalysis and spectroscopy.

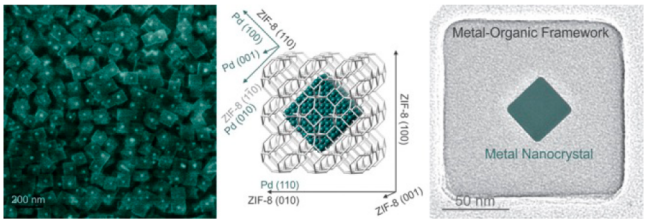

Figure 7. SEM image of Pd nanocubes individually incased in single crystalline ZIF-8 particles. Schematic shows the alignment between the Pd core and ZIF-8 shell. TEM image of Pd@ZIF-8 shows the accordance with the illustration. (Reprinted with permission from ref 182. Copyright ©American Chemical Society 2014.)

4.3. Postsynthetic Modifications of MOF. Postsynthetic modification (PSM) and linker exchange have become powerful tools to engineer MOFs for catalysis.[62,137,188–197] We envision

dx.doi.org/10.1021/cs5012662 | ACS Catal. 2014, 4, 4409–4419

that such postsynthetic operations will form a basis to extend metal@MOF core−shell composites to increasingly sophisticated applications that rely on tailored chemical functionality in the pores. PSM adapts to MOFs strategies developed for zeolites and mesoporous silica, which have long been functionalized after synthesis both covalently, by the organic derivatization of surface silanols, and datively, by the coordination of transition metals to deprotonated siloxides. MOFs offer even more versatility for postsynthetic transformations due to their functionalizable organic linkers and more diverse coordination chemistry.[195] The most common chemical handle for covalent MOF PSM is amines, especially 2-aminoterephthalate for MOF-5 and UiO-66. Coordinative PSM uses the unoccupied sites found in many MOFs such as HKUST-1 and MIL-101 to datively bind functional molecules. Postsynthetic linker exchange has been demonstrated in a great variety of MOFs and can be a route to frameworks that cannot be synthesized *de novo*.[191] Our group recently discovered evidence for the formation of enlarged pore apertures by linker dissociation during MOF linker exchange, as demonstrated by the postsynthetic encapsulation of species much larger than the pore aperture of ZIF-8 (Figure 8).[161] It was demonstrated by

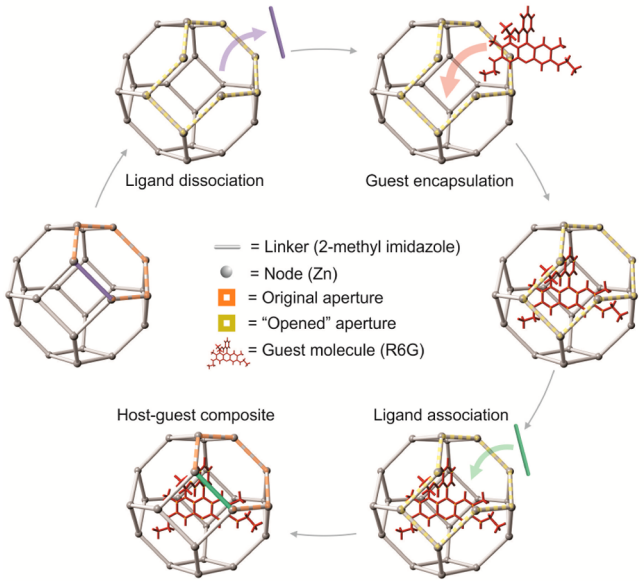

Figure 8. Schematic of encapsulation of molecules larger than aperture size during dissociative linker exchange. (Reprinted with permission from ref 157. Copyright ©American Chemical Society 2014.)

kinetic studies that linker exchange proceeds by a competition between associative and dissociative linker exchange mechanisms, and guest encapsulation was enhanced under conditions that favored the dissociative pathway. This phenomenon could aid the postsynthetic loading of active guests into metal@MOF composites for added functionality.

PSM and linker exchange have the potential to enhance the performance of metal@MOF structures for catalysis by adding functionality that could (1) dock substrates by molecular recognition,[90] (2) act as acid/base catalytic sites, or (3) bind transition metals for tandem catalysis with the metal core. Since many functional groups of interest for these purposes bind transition metals, they may be considered a nuisance during metal nanocrystal encapsulation, during which they could interfere with proper placement in the MOF crystals and/or be metalated and hence not available for further chemistry. Linker exchange allows MOF synthesis and linker functionalization to be decoupled and therefore is an attractive route for adding functionality to the linkers of metal@MOF nanoparticle composites.

5. CONCLUSION AND OUTLOOK

In the past decades, significant progress has been made in the combination of metal nanocatalysts and nanoporous materials. From the stiff and solid zeolite to the flexible and modifiable MOF, scientists have developed advanced materials that can be integrated with metal catalysts. Various synthetic strategies for incorporating metal nanoparticles in nanoporous materials (i.e., MOFs) have also been developed, and many applications of the composite materials in heterogeneous catalysis have been demonstrated. As one of the most promising materials, MOFs have been intensively studied, and the encapsulation of metal nanoparticles into MOFs was thoroughly discussed. Different types of catalytic reactions applications were shown to demonstrate the potential of metal@MOF composite materials. The promise of this class of materials for heterogeneous catalysis will be promoted by further mechanistic studies of their action and development of applications.

AUTHOR INFORMATION

Corresponding Author

*E-mail: frank.tsung@bc.edu.

Notes

The authors declare no competing financial interest.

ACKNOWLEDGMENTS

Acknowledgment is made to the donors of the American Chemical Society Petroleum Research Fund. The authors thank the support from Boston College.

REFERENCES

(1) George, S. M. *Chem. Rev.* **1995**, *95*, 475.
(2) Zhang, S.; Nguyen, L.; Zhu, Y.; Zhan, S.; Tsung, C.-K.; Tao, F. *Acc. Chem. Res.* **2013**, *46*, 1731.
(3) Narayanan, R.; El-Sayed, M. A. *J. Phys. Chem. B* **2005**, *109*, 12663.
(4) De Rogatis, L.; Cargnello, M.; Gombac, V.; Lorenzut, B.; Montini, T.; Fornasiero, P. *ChemSusChem* **2010**, *3*, 24.
(5) Liu, S.; Han, M.-Y. *Chem. − Asian J.* **2010**, *5*, 36.
(6) Guerrero-Martínez, A.; Pérez-Juste, J.; Liz-Marzán, L. M. *Adv. Mater.* **2010**, *22*, 1182.
(7) Sun, X.; Li, Y. *Angew. Chem., Int. Ed.* **2004**, *43*, 597.
(8) Ikeda, S.; Ishino, S.; Harada, T.; Okamoto, N.; Sakata, T.; Mori, H.; Kuwabata, S.; Torimoto, T.; Matsumura, M. *Angew. Chem., Int. Ed.* **2006**, *45*, 7063.
(9) Lee, J.; Kim, J.; Hyeon, T. *Adv. Mater.* **2006**, *18*, 2073.
(10) Liu, R.; Mahurin, S. M.; Li, C.; Unocic, R. R.; Idrobo, J. C.; Gao, H.; Pennycook, S. J.; Dai, S. *Angew. Chem., Int. Ed.* **2011**, *50*, 6799.
(11) Teng, X.; Black, D.; Watkins, N. J.; Gao, Y.; Yang, H. *Nano Lett.* **2003**, *3*, 261.
(12) Zhang, N.; Liu, S.; Xu, Y.-J. *Nanoscale* **2012**, *4*, 2227.
(13) Suh, W. H.; Jang, A. R.; Suh, Y. H.; Suslick, K. S. *Adv. Mater.* **2006**, *18*, 1832.
(14) Sun, H.; He, J.; Wang, J.; Zhang, S.-Y.; Liu, C.; Sritharan, T.; Mhaisalkar, S.; Han, M.-Y.; Wang, D.; Chen, H. *J. Am. Chem. Soc.* **2013**, *135*, 9099.
(15) Li, G.; Tang, Z. *Nanoscale* **2014**, *6*, 3995.
(16) Zhang, Q.; Lee, I.; Ge, J.; Zaera, F.; Yin, Y. *Adv. Funct. Mater.* **2010**, *20*, 2201.
(17) Wang, H.; Chen, L.; Feng, Y.; Chen, H. *Acc. Chem. Res.* **2013**, *46*, 1636.

(18) Bell, A. T. *Science* **2003**, *299*, 1688.
(19) Lee, H.; Habas, S. E.; Kweskin, S.; Butcher, D.; Somorjai, G. A.; Yang, P. *Angew. Chem., Int. Ed.* **2006**, *45*, 7824.
(20) Bratlie, K. M.; Lee, H.; Komvopoulos, K.; Yang, P.; Somorjai, G. A. *Nano Lett.* **2007**, *7*, 3097.
(21) Habas, S. E.; Lee, H.; Radmilovic, V.; Somorjai, G. A.; Yang, P. *Nat. Mater.* **2007**, *6*, 692.
(22) Xiong, Y.; Wiley, B. J.; Xia, Y. *Angew. Chem., Int. Ed.* **2007**, *46*, 7157.
(23) Chen, J.; Lim, B.; Lee, E. P.; Xia, Y. *Nano Today* **2009**, *4*, 81.
(24) Wang, D.; Li, Y. *Adv. Mater.* **2011**, *23*, 1044.
(25) Gu, J.; Zhang, Y.-W.; Tao, F. *Chem. Soc. Rev.* **2012**, *41*, 8050.
(26) Wang, C.; Markovic, N. M.; Stamenkovic, V. R. *ACS Catal.* **2012**, *2*, 891.
(27) Wu, J.; Li, P.; Pan, Y.-T.; Warren, S.; Yin, X.; Yang, H. *Chem. Soc. Rev.* **2012**, *41*, 8066.
(28) Yu, W.; Porosoff, M. D.; Chen, J. G. *Chem. Rev.* **2012**, *112*, 5780.
(29) Zhang, H.; Jin, M.; Xia, Y. *Chem. Soc. Rev.* **2012**, *41*, 8035.
(30) Cargnello, M.; Fornasiero, P.; Gorte, R. J. *ChemPhysChem* **2013**, *14*, 3869.
(31) Cui, C.-H.; Yu, S.-H. *Acc. Chem. Res.* **2013**, *46*, 1427.
(32) Guo, S.; Zhang, S.; Sun, S. *Angew. Chem., Int. Ed.* **2013**, *52*, 8526.
(33) Zhang, X.; Yin, H.; Wang, J.; Chang, L.; Gao, Y.; Liu, W.; Tang, Z. *Nanoscale* **2013**, *5*, 8392.
(34) Wu, Y.; Wang, D.; Li, Y. *Chem. Soc. Rev.* **2014**, *43*, 2112.
(35) Zhang, Z. C.; Xu, B.; Wang, X. *Chem. Soc. Rev.* **2014**, *43*, 7870.
(36) Polshettiwar, V.; Luque, R.; Fihri, A.; Zhu, H.; Bouhrara, M.; Basset, J.-M. *Chem. Rev.* **2011**, *111*, 3036.
(37) Jia, C.-J.; Schuth, F. *Phys. Chem. Chem. Phys.* **2011**, *13*, 2457.
(38) Lohse, S. E.; Murphy, C. J. *J. Am. Chem. Soc.* **2012**, *134*, 15607.
(39) Lal, S.; Clare, S. E.; Halas, N. J. *Acc. Chem. Res.* **2008**, *41*, 1842.
(40) Motl, N. E.; Smith, A. F.; DeSantis, C. J.; Skrabalak, S. E. *Chem. Soc. Rev.* **2014**, *43*, 3823.
(41) Li, J. F.; Huang, Y. F.; Ding, Y.; Yang, Z. L.; Li, S. B.; Zhou, X. S.; Fan, F. R.; Zhang, W.; Zhou, Z. Y.; WuDe, Y.; Ren, B.; Wang, Z. L.; Tian, Z. Q. *Nature* **2010**, *464*, 392.
(42) Schartl, W. *Nanoscale* **2010**, *2*, 829.
(43) Ghosh Chaudhuri, R.; Paria, S. *Chem. Rev.* **2011**, *112*, 2373.
(44) Liu, J.; Qiao, S. Z.; Chen, J. S.; Lou, X. W.; Xing, X.; Lu, G. Q. *Chem. Commun.* **2011**, *47*, 12578.
(45) Wei, S.; Wang, Q.; Zhu, J.; Sun, L.; Lin, H.; Guo, Z. *Nanoscale* **2011**, *3*, 4474.
(46) Zhang, Q.; Lee, I.; Joo, J. B.; Zaera, F.; Yin, Y. *Acc. Chem. Res.* **2012**, *46*, 1816.
(47) Mitsudome, T.; Kaneda, K. *ChemCatChem* **2013**, *5*, 1681.
(48) Zeng, H. C. *Acc. Chem. Res.* **2012**, *46*, 226.
(49) Zheng, F.; Wong, W.-T.; Yung, K.-F. *Nano Res.* **2014**, *7*, 410.
(50) Guan, B.; Wang, T.; Zeng, S.; Wang, X.; An, D.; Wang, D.; Cao, Y.; Ma, D.; Liu, Y.; Huo, Q. *Nano Res.* **2014**, *7*, 246.
(51) Metin, Ö.; Ho, S.; Alp, C.; Can, H.; Mankin, M.; Gültekin, M.; Chi, M.; Sun, S. *Nano Res.* **2013**, *6*, 10.
(52) Aranishi, K.; Jiang, H.-L.; Akita, T.; Haruta, M.; Xu, Q. *Nano Res.* **2011**, *4*, 1233.
(53) Joo, S. H.; Park, J. Y.; Tsung, C.-K.; Yamada, Y.; Yang, P.; Somorjai, G. A. *Nat. Mater.* **2009**, *8*, 126.
(54) Guttel, R.; Paul, M.; Schuth, F. *Chem. Commun.* **2010**, *46*, 895.
(55) Li, J.; Zeng, H. C. *Angew. Chem., Int. Ed.* **2005**, *44*, 4342.
(56) Mitsudome, T.; Mikami, Y.; Matoba, M.; Mizugaki, T.; Jitsukawa, K.; Kaneda, K. *Angew. Chem., Int. Ed.* **2012**, *51*, 136.
(57) Chen, C.; Fang, X.; Wu, B.; Huang, L.; Zheng, N. *ChemCatChem* **2012**, *4*, 1578.
(58) Li, H.; Eddaoudi, M.; O'Keeffe, M.; Yaghi, O. M. *Nature* **1999**, *402*, 276.
(59) Eddaoudi, M.; Moler, D. B.; Li, H.; Chen, B.; Reineke, T. M.; O'Keeffe, M.; Yaghi, O. M. *Acc. Chem. Res.* **2001**, *34*, 319.
(60) James, S. L. *Chem. Soc. Rev.* **2003**, *32*, 276.
(61) Park, K. S.; Ni, Z.; Côté, A. P.; Choi, J. Y.; Huang, R.; Uribe-Romo, F. J.; Chae, H. K.; O'Keeffe, M.; Yaghi, O. M. *Proc. Natl. Acad. Sci. U. S. A.* **2006**, *103*, 10186.
(62) Cohen, S. M. *Chem. Sci.* **2010**, *1*, 32.
(63) Farha, O. K.; Hupp, J. T. *Acc. Chem. Res.* **2010**, *43*, 1166.
(64) Janiak, C.; Vieth, J. K. *New J. Chem.* **2010**, *34*, 2366.
(65) Stock, N.; Biswas, S. *Chem. Rev.* **2011**, *112*, 933.
(66) Zhou, H.-C.; Long, J. R.; Yaghi, O. M. *Chem. Rev.* **2012**, *112*, 673.
(67) Furukawa, H.; Cordova, K. E.; O'Keeffe, M.; Yaghi, O. M. *Science* **2013**, *341*, 1230444 .
(68) Meek, S. T.; Greathouse, J. A.; Allendorf, M. D. *Adv. Mater.* **2011**, *23*, 249.
(69) Li, Y.; Yang, R. T. *J. Am. Chem. Soc.* **2005**, *128*, 726.
(70) Rowsell, J. L. C.; Yaghi, O. M. *Angew. Chem., Int. Ed.* **2005**, *44*, 4670.
(71) Li, Y.; Yang, R. T. *J. Am. Chem. Soc.* **2006**, *128*, 8136.
(72) Cheon, Y. E.; Suh, M. P. *Angew. Chem., Int. Ed.* **2009**, *48*, 2899.
(73) Murray, L. J.; Dinca, M.; Long, J. R. *Chem. Soc. Rev.* **2009**, *38*, 1294.
(74) Li, S.-L.; Xu, Q. *Energy Environ. Sci.* **2013**, *6*, 1656.
(75) Li, G.; Kobayashi, H.; Taylor, J. M.; Ikeda, R.; Kubota, Y.; Kato, K.; Takata, M.; Yamamoto, T.; Toh, S.; Matsumura, S.; Kitagawa, H. *Nat. Mater.* **2014**, *13*, 802.
(76) Rosi, N. L.; Eckert, J.; Eddaoudi, M.; Vodak, D. T.; Kim, J.; O'Keeffe, M.; Yaghi, O. M. *Science* **2003**, *300*, 1127.
(77) Millward, A. R.; Yaghi, O. M. *J. Am. Chem. Soc.* **2005**, *127*, 17998.
(78) Zou, R.; Abdel-Fattah, A. I.; Xu, H.; Zhao, Y.; Hickmott, D. D. *CrystEngComm* **2010**, *12*, 1337.
(79) Seo, J. S.; Whang, D.; Lee, H.; Jun, S. I.; Oh, J.; Jeon, Y. J.; Kim, K. *Nature* **2000**, *404*, 982.
(80) Li, J.-R.; Kuppler, R. J.; Zhou, H.-C. *Chem. Soc. Rev.* **2009**, *38*, 1477.
(81) Britt, D.; Furukawa, H.; Wang, B.; Glover, T. G.; Yaghi, O. M. *Proc. Natl. Acad. Sci. U. S. A.* **2009**, *106*, 20637.
(82) Jiang, H.-L.; Tatsu, Y.; Lu, Z.-H.; Xu, Q. *J. Am. Chem. Soc.* **2010**, *132*, 5586.
(83) Lu, Z.-Z.; Zhang, R.; Li, Y.-Z.; Guo, Z.-J.; Zheng, H.-G. *J. Am. Chem. Soc.* **2011**, *133*, 4172.
(84) Achmann, S.; Hagen, G.; Kita, J.; Malkowsky, I.; Kiener, C.; Moos, R. *Sensors* **2009**, *9*, 1574.
(85) Kreno, L. E.; Hupp, J. T.; Van Duyne, R. P. *Anal. Chem.* **2010**, *82*, 8042.
(86) Della Rocca, J.; Liu, D.; Lin, W. *Acc. Chem. Res.* **2011**, *44*, 957.
(87) Zhuang, J.; Kuo, C. H.; Chou, L. Y.; Liu, D. Y.; Weerapana, E.; Tsung, C. K. *ACS Nano* **2014**, *8*, 2812.
(88) An, J.; Geib, S. J.; Rosi, N. L. *J. Am. Chem. Soc.* **2009**, *131*, 8376.
(89) Huxford, R. C.; Della Rocca, J.; Lin, W. *Curr. Opin. Chem. Biol.* **2010**, *14*, 262.
(90) Li, Q.; Zhang, W.; Miljanić, O. Š.; Sue, C.-H.; Zhao, Y.-L.; Liu, L.; Knobler, C. B.; Stoddart, J. F.; Yaghi, O. M. *Science* **2009**, *325*, 855.
(91) Alkordi, M. H.; Liu, Y.; Larsen, R. W.; Eubank, J. F.; Eddaoudi, M. *J. Am. Chem. Soc.* **2008**, *130*, 12639.
(92) Farrusseng, D.; Aguado, S.; Pinel, C. *Angew. Chem., Int. Ed.* **2009**, *48*, 7502.
(93) Lee, J.; Farha, O. K.; Roberts, J.; Scheidt, K. A.; Nguyen, S. T.; Hupp, J. T. *Chem. Soc. Rev.* **2009**, *38*, 1450.
(94) Corma, A.; García, H.; Llabrés i Xamena, F. X. *Chem. Rev.* **2010**, *110*, 4606.
(95) Yoon, M.; Srirambalaji, R.; Kim, K. *Chem. Rev.* **2011**, *112*, 1196.
(96) Mueller, U.; Schubert, M.; Teich, F.; Puetter, H.; Schierle-Arndt, K.; Pastre, J. *J. Mater. Chem.* **2006**, *16*, 626.
(97) Dhakshinamoorthy, A.; Alvaro, M.; Garcia, H. *Chem. Commun.* **2012**, *48*, 11275.
(98) Meilikhov, M.; Yusenko, K.; Esken, D.; Turner, S.; Van Tendeloo, G.; Fischer, R. A. *Eur. J. Inorg. Chem.* **2010**, *2010*, 3701.
(99) Dhakshinamoorthy, A.; Garcia, H. *Chem. Soc. Rev.* **2012**, *41*, 5262.

(100) Doherty, C. M.; Buso, D.; Hill, A. J.; Furukawa, S.; Kitagawa, S.; Falcaro, P. *Acc. Chem. Res.* **2013**, *47*, 396.
(101) Foo, M. L.; Matsuda, R.; Kitagawa, S. *Chem. Mater.* **2013**, *26*, 310.
(102) Moon, H. R.; Lim, D.-W.; Suh, M. P. *Chem. Soc. Rev.* **2013**, *42*, 1807.
(103) Zhu, Q. L.; Xu, Q. *Chem. Soc. Rev.* **2014**, *43*, 5468.
(104) Liu, Y.; Tang, Z. *Adv. Mater.* **2013**, *25*, 5819.
(105) Aijaz, A.; Xu, Q. *J. Phys. Chem. Lett.* **2014**, *5*, 1400.
(106) Huang, X.; Zheng, B.; Liu, Z.; Tan, C.; Liu, J.; Chen, B.; Li, H.; Chen, J.; Zhang, X.; Fan, Z.; Zhang, W.; Guo, Z.; Huo, F.; Yang, Y.; Xie, L.-H.; Huang, W.; Zhang, H. *ACS Nano* **2014**, *8*, 8695.
(107) Huang, Y.; Zhang, Y.; Chen, X.; Wu, D.; Yi, Z.; Cao, R. *Chem. Commun.* **2014**, *50*, 10115.
(108) Cao, N.; Yang, L.; Dai, H.; Liu, T.; Su, J.; Wu, X.; Luo, W.; Cheng, G. *Inorg. Chem.* **2014**, *53*, 10122−10128.
(109) Zhang, W.; Lu, G.; Cui, C.; Liu, Y.; Li, S.; Yan, W.; Xing, C.; Chi, Y. R.; Yang, Y.; Huo, F. *Adv. Mater.* **2014**, *26*, 4056.
(110) Jin, S.; Son, H.-J.; Farha, O. K.; Wiederrecht, G. P.; Hupp, J. T. *J. Am. Chem. Soc.* **2013**, *135*, 955.
(111) Buso, D.; Jasieniak, J.; Lay, M. D. H.; Schiavuta, P.; Scopece, P.; Laird, J.; Amenitsch, H.; Hill, A. J.; Falcaro, P. *Small* **2012**, *8*, 80.
(112) Esken, D.; Turner, S.; Wiktor, C.; Kalidindi, S. B.; Van Tendeloo, G.; Fischer, R. A. *J. Am. Chem. Soc.* **2011**, *133*, 16370.
(113) Sun, C.-Y.; Liu, S.-X.; Liang, D.-D.; Shao, K.-Z.; Ren, Y.-H.; Su, Z.-M. *J. Am. Chem. Soc.* **2009**, *131*, 1883.
(114) Ma, F.-J.; Liu, S.-X.; Sun, C.-Y.; Liang, D.-D.; Ren, G.-J.; Wei, F.; Chen, Y.-G.; Su, Z.-M. *J. Am. Chem. Soc.* **2011**, *133*, 4178.
(115) Song, J.; Luo, Z.; Britt, D. K.; Furukawa, H.; Yaghi, O. M.; Hardcastle, K. I.; Hill, C. L. *J. Am. Chem. Soc.* **2011**, *133*, 16839.
(116) Distefano, G.; Suzuki, H.; Tsujimoto, M.; Isoda, S.; Bracco, S.; Comotti, A.; Sozzani, P.; Uemura, T.; Kitagawa, S. *Nat. Chem.* **2013**, *5*, 335.
(117) Lee, H. J.; Cho, W.; Oh, M. *Chem. Commun.* **2012**, *48*, 221.
(118) Jo, C.; Lee, H. J.; Oh, M. *Adv. Mater.* **2011**, *23*, 1716.
(119) Xing, L.; Zheng, H.; Cao, Y.; Che, S. *Adv. Mater.* **2012**, *24*, 6433.
(120) Liu, N.; Yao, Y.; Cha, J.; McDowell, M.; Han, Y.; Cui, Y. *Nano Res.* **2012**, *5*, 109.
(121) Yang, S. J.; Choi, J. Y.; Chae, H. K.; Cho, J. H.; Nahm, K. S.; Park, C. R. *Chem. Mater.* **2009**, *21*, 1893.
(122) Xiang, Z.; Hu, Z.; Cao, D.; Yang, W.; Lu, J.; Han, B.; Wang, W. *Angew. Chem., Int. Ed.* **2011**, *50*, 491.
(123) Liu, W.-L.; Lo, S.-H.; Singco, B.; Yang, C.-C.; Huang, H.-Y.; Lin, C.-H. *J. Mater. Chem. B* **2013**, *1*, 928.
(124) Lykourinou, V.; Chen, Y.; Wang, X.-S.; Meng, L.; Hoang, T.; Ming, L.-J.; Musselman, R. L.; Ma, S. *J. Am. Chem. Soc.* **2011**, *133*, 10382.
(125) Liu, J.; Strachan, D. M.; Thallapally, P. K. *Chem. Commun.* **2014**, *50*, 466.
(126) He, L.; Liu, Y.; Liu, J.; Xiong, Y.; Zheng, J.; Liu, Y.; Tang, Z. *Angew. Chem., Int. Ed.* **2013**, *52*, 3741.
(127) Sugikawa, K.; Nagata, S.; Furukawa, Y.; Kokado, K.; Sada, K. *Chem. Mater.* **2013**, *25*, 2565.
(128) Khaletskaya, K.; Reboul, J.; Meilikhov, M.; Nakahama, M.; Diring, S.; Tsujimoto, M.; Isoda, S.; Kim, F.; Kamei, K.-i.; Fischer, R. A.; Kitagawa, S.; Furukawa, S. *J. Am. Chem. Soc.* **2013**, *135*, 10998.
(129) Smit, B.; Maesen, T. L. M. *Nature* **2008**, *451*, 671.
(130) Gounder, R.; Iglesia, E. *Chem. Commun.* **2013**, *49*, 3491.
(131) Wang, P.; Zhao, J.; Li, X.; Yang, Y.; Yang, Q.; Li, C. *Chem. Commun.* **2013**, *49*, 3330.
(132) Corma, A.; Garcia, H. *Eur. J. Inorg. Chem.* **2004**, *2004*, 1143.
(133) Hermes, S.; Schröter, M.-K.; Schmid, R.; Khodeir, L.; Muhler, M.; Tissler, A.; Fischer, R. W.; Fischer, R. A. *Angew. Chem., Int. Ed.* **2005**, *44*, 6237.
(134) Muller, M.; Lebedev, O. I.; Fischer, R. A. *J. Mater. Chem.* **2008**, *18*, 5274.
(135) Schröder, F.; Esken, D.; Cokoja, M.; van den Berg, M. W. E.; Lebedev, O. I.; Van Tendeloo, G.; Walaszek, B.; Buntkowsky, G.; Limbach, H.-H.; Chaudret, B.; Fischer, R. A. *J. Am. Chem. Soc.* **2008**, *130*, 6119.
(136) Esken, D.; Zhang, X.; Lebedev, O. I.; Schroder, F.; Fischer, R. A. *J. Mater. Chem.* **2009**, *19*, 1314.
(137) Meilikhov, M.; Yusenko, K.; Fischer, R. A. *J. Am. Chem. Soc.* **2009**, *131*, 9644.
(138) Schröder, F.; Henke, S.; Zhang, X.; Fischer, R. A. *Eur. J. Inorg. Chem.* **2009**, *2009*, 3131.
(139) Esken, D.; Turner, S.; Lebedev, O. I.; Van Tendeloo, G.; Fischer, R. A. *Chem. Mater.* **2010**, *22*, 6393.
(140) Meilikhov, M.; Yusenko, K.; Torrisi, A.; Jee, B.; Mellot-Draznieks, C.; Pöppl, A.; Fischer, R. A. *Angew. Chem., Int. Ed.* **2010**, *49*, 6212.
(141) Ishida, T.; Nagaoka, M.; Akita, T.; Haruta, M. *Chem. − Eur. J.* **2008**, *14*, 8456.
(142) Jiang, H.-L.; Liu, B.; Akita, T.; Haruta, M.; Sakurai, H.; Xu, Q. *J. Am. Chem. Soc.* **2009**, *131*, 11302.
(143) Jiang, H.-L.; Lin, Q.-P.; Akita, T.; Liu, B.; Ohashi, H.; Oji, H.; Honma, T.; Takei, T.; Haruta, M.; Xu, Q. *Chem. − Eur. J.* **2011**, *17*, 78.
(144) Gu, X.; Lu, Z.-H.; Jiang, H.-L.; Akita, T.; Xu, Q. *J. Am. Chem. Soc.* **2011**, *133*, 11822.
(145) Jiang, H.-L.; Akita, T.; Ishida, T.; Haruta, M.; Xu, Q. *J. Am. Chem. Soc.* **2011**, *133*, 1304.
(146) Aijaz, A.; Karkamkar, A.; Choi, Y. J.; Tsumori, N.; Rönnebro, E.; Autrey, T.; Shioyama, H.; Xu, Q. *J. Am. Chem. Soc.* **2012**, *134*, 13926.
(147) Zhu, Q.-L.; Li, J.; Xu, Q. *J. Am. Chem. Soc.* **2013**, *135*, 10210.
(148) Aijaz, A.; Akita, T.; Tsumori, N.; Xu, Q. *J. Am. Chem. Soc.* **2013**, *135*, 16356.
(149) Sugikawa, K.; Furukawa, Y.; Sada, K. *Chem. Mater.* **2011**, *23*, 3132.
(150) Tsuruoka, T.; Kawasaki, H.; Nawafune, H.; Akamatsu, K. *ACS Appl. Mater. Interfaces* **2011**, *3*, 3788.
(151) Lu, G.; Li, S.; Guo, Z.; Farha, O. K.; Hauser, B. G.; Qi, X.; Wang, Y.; Wang, X.; Han, S.; Liu, X.; DuChene, J. S.; Zhang, H.; Zhang, Q.; Chen, X.; Ma, J.; Loo, S. C. J.; Wei, W. D.; Yang, Y.; Hupp, J. T.; Huo, F. *Nat. Chem.* **2012**, *4*, 310.
(152) Zhao, M.; Deng, K.; He, L.; Liu, Y.; Li, G.; Zhao, H.; Tang, Z. *J. Am. Chem. Soc.* **2014**, *136*, 1738.
(153) Valden, M.; Lai, X.; Goodman, D. W. *Science* **1998**, *281*, 1647.
(154) El-Shall, M. S.; Abdelsayed, V.; Khder, A. E. R. S.; Hassan, H. M. A.; El-Kaderi, H. M.; Reich, T. E. *J. Mater. Chem.* **2009**, *19*, 7625.
(155) Kuo, C.-H.; Tang, Y.; Chou, L.-Y.; Sneed, B. T.; Brodsky, C. N.; Zhao, Z.; Tsung, C.-K. *J. Am. Chem. Soc.* **2012**, *134*, 14345.
(156) Zhang, C.; Lively, R. P.; Zhang, K.; Johnson, J. R.; Karvan, O.; Koros, W. J. *J. Phys. Chem. Lett.* **2012**, *3*, 2130.
(157) Na, K.; Choi, K. M.; Yaghi, O. M.; Somorjai, G. A. *Nano Lett.* **2014**, *14*, 5979−5983.
(158) Cavka, J. H.; Jakobsen, S.; Olsbye, U.; Guillou, N.; Lamberti, C.; Bordiga, S.; Lillerud, K. P. *J. Am. Chem. Soc.* **2008**, *130*, 13850.
(159) Greathouse, J. A.; Allendorf, M. D. *J. Am. Chem. Soc.* **2006**, *128*, 10678.
(160) Kim, M.; Cahill, J. F.; Fei, H.; Prather, K. A.; Cohen, S. M. *J. Am. Chem. Soc.* **2012**, *134*, 18082.
(161) Morabito, J. V.; Chou, L.-Y.; Li, Z.; Manna, C. M.; Petroff, C. A.; Kyada, R.; Palomba, J. M.; Byers, J. A.; Tsung, C.-K. *J. Am. Chem. Soc.* **2014**, *136*, 12540.
(162) Yuan, B.; Pan, Y.; Li, Y.; Yin, B.; Jiang, H. *Angew. Chem., Int. Ed.* **2010**, *49*, 4054.
(163) Pan, Y.; Yuan, B.; Li, Y.; He, D. *Chem. Commun.* **2010**, *46*, 2280.
(164) Hwang, Y. K.; Hong, D.-Y.; Chang, J.-S.; Jhung, S. H.; Seo, Y.-K.; Kim, J.; Vimont, A.; Daturi, M.; Serre, C.; Férey, G. *Angew. Chem., Int. Ed.* **2008**, *47*, 4144.
(165) Kandiah, M.; Nilsen, M. H.; Usseglio, S.; Jakobsen, S.; Olsbye, U.; Tilset, M.; Larabi, C.; Quadrelli, E. A.; Bonino, F.; Lillerud, K. P. *Chem. Mater.* **2010**, *22*, 6632.
(166) Guo, Z.; Xiao, C.; Maligal-Ganesh, R. V.; Zhou, L.; Goh, T. W.; Li, X.; Tesfagaber, D.; Thiel, A.; Huang, W. *ACS Catal.* **2014**, *4*, 1340.

(167) Nicolaou, K. C.; Edmonds, D. J.; Bulger, P. G. *Angew. Chem., Int. Ed.* **2006**, *45*, 7134.
(168) Li, X.; Guo, Z.; Xiao, C.; Goh, T. W.; Tesfagaber, D.; Huang, W. *ACS Catal.* **2014**, 3490.
(169) Zhang, T.; Lin, W. *Chem. Soc. Rev.* **2014**, *43*, 5982.
(170) Son, H.-J.; Jin, S.; Patwardhan, S.; Wezenberg, S. J.; Jeong, N. C.; So, M.; Wilmer, C. E.; Sarjeant, A. A.; Schatz, G. C.; Snurr, R. Q.; Farha, O. K.; Wiederrecht, G. P.; Hupp, J. T. *J. Am. Chem. Soc.* **2012**, *135*, 862.
(171) Lee, C. Y.; Farha, O. K.; Hong, B. J.; Sarjeant, A. A.; Nguyen, S. T.; Hupp, J. T. *J. Am. Chem. Soc.* **2011**, *133*, 15858.
(172) Wang, C.; deKrafft, K. E.; Lin, W. *J. Am. Chem. Soc.* **2012**, *134*, 7211.
(173) Ma, S.; Sun, D.; Ambrogio, M.; Fillinger, J. A.; Parkin, S.; Zhou, H.-C. *J. Am. Chem. Soc.* **2007**, *129*, 1858.
(174) Dincă, M.; Long, J. R. *J. Am. Chem. Soc.* **2007**, *129*, 11172.
(175) Mulfort, K. L.; Hupp, J. T. *J. Am. Chem. Soc.* **2007**, *129*, 9604.
(176) Zlotea, C.; Campesi, R.; Cuevas, F.; Leroy, E.; Dibandjo, P.; Volkringer, C.; Loiseau, T.; Férey, G.; Latroche, M. *J. Am. Chem. Soc.* **2010**, *132*, 2991.
(177) Sabo, M.; Henschel, A.; Frode, H.; Klemm, E.; Kaskel, S. *J. Mater. Chem.* **2007**, *17*, 3827.
(178) Park, J. C.; Bang, J. U.; Lee, J.; Ko, C. H.; Song, H. *J. Mater. Chem.* **2010**, *20*, 1239.
(179) Park, J.; Song, H. *Nano Res.* **2011**, *4*, 33.
(180) Liu, Y.; Zhang, W.; Li, S.; Cui, C.; Wu, J.; Chen, H.; Huo, F. *Chem. Mater.* **2013**, *26*, 1119.
(181) Zhang, Z.; Chen, Y.; Xu, X.; Zhang, J.; Xiang, G.; He, W.; Wang, X. *Angew. Chem., Int. Ed.* **2014**, *53*, 429.
(182) Wu, X.-J.; Xu, D. *Adv. Mater.* **2010**, *22*, 1516.
(183) Sindoro, M.; Granick, S. *J. Am. Chem. Soc.* **2014**, *136*, 13471.
(184) Zaera, F. *Chem. Rev.* **2012**, *112*, 2920.
(185) Ameloot, R.; Vermoortele, F.; Vanhove, W.; Roeffaers, M. B. J.; Sels, B. F.; De Vos, D. E. *Nat. Chem.* **2011**, *3*, 382.
(186) Li, S.; Shi, W.; Lu, G.; Li, S.; Loo, S. C. J.; Huo, F. *Adv. Mater.* **2012**, *24*, 5954.
(187) Hu, P.; Zhuang, J.; Chou, L. Y.; Lee, H. K.; Ling, X. Y.; Chuang, Y. C.; Tsung, C. K. *J. Am. Chem. Soc.* **2014**, *136*, 10561.
(188) Deria, P.; Mondloch, J. E.; Karagiaridi, O.; Bury, W.; Hupp, J. T.; Farha, O. K. *Chem. Soc. Rev.* **2014**, *43*, 5896.
(189) Tanabe, K. K.; Cohen, S. M. *Chem. Soc. Rev.* **2011**, *40*, 498.
(190) Karagiaridi, O.; Bury, W.; Mondloch, J. E.; Hupp, J. T.; Farha, O. K. *Angew. Chem., Int. Ed.* **2014**, *53*, 4530.
(191) Karagiaridi, O.; Lalonde, M. B.; Bury, W.; Sarjeant, A. A.; Farha, O. K.; Hupp, J. T. *J. Am. Chem. Soc.* **2012**, *134*, 18790.
(192) Brozek, C. K.; Dinca, M. *Chem. Soc. Rev.* **2014**, *43*, 5456.
(193) Takaishi, S.; DeMarco, E. J.; Pellin, M. J.; Farha, O. K.; Hupp, J. T. *Chem. Sci.* **2013**, *4*, 1509.
(194) Farha, O. K.; Shultz, A. M.; Sarjeant, A. A.; Nguyen, S. T.; Hupp, J. T. *J. Am. Chem. Soc.* **2011**, *133*, 5652.
(195) Cohen, S. M. *Chem. Rev.* **2011**, *112*, 970.
(196) Banerjee, M.; Das, S.; Yoon, M.; Choi, H. J.; Hyun, M. H.; Park, S. M.; Seo, G.; Kim, K. *J. Am. Chem. Soc.* **2009**, *131*, 7524.
(197) Mondloch, J. E.; Karagiaridi, O.; Farha, O. K.; Hupp, J. T. *CrystEngComm* **2013**, *15*, 9258.

dx.doi.org/10.1021/cs5012662 | *ACS Catal.* 2014, 4, 4409−4419